 DOI 10.1515/htmp-2012-0077 — High Temp. Mater. Proc. 2012; 31(4-5): 421–430

M. Hasegawa*, Y. Kashiwaya and M. Iwase

Thermodynamic Properties of Solid Solutions between Di-calcium Silicate and Tri-calcium Phosphate

Abstract: For a better understanding of phosphorus removal from hot metal, the Gibbs free energies of solid solutions between di-calcium silicate and tri-calcium phosphate were derived through applications of solutions models. The regular solution model with the parameters determined in this study gave the activities of the components thermodynamically consistent with the literature data and the phase diagrams.

Keywords: di-calcium silicate, tri-calcium phosphate, solid solution, dephosphorization

PACS® (2010). 82.60.-s

***Corresponding author: M. Hasegawa:** Department of Energy Science and Technology, Kyoto University, Kyoto 606-8501, Japan
E-mail: hasegawa@energy.kyoto-u.ac.jp
Y. Kashiwaya: Department of Energy Science and Technology, Kyoto University, Kyoto 606-8501, Japan
M. Iwase: Department of Energy Science and Technology, Kyoto University, Kyoto 606-8501, Japan

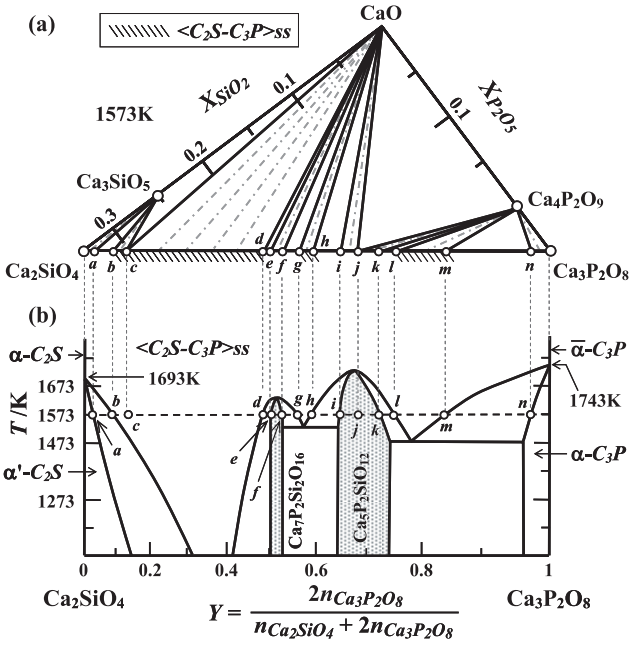

Fig. 1: (a) Iso-thermal section of the ternary system CaO-SiO_2-P_2O_5 near the CaO apex at 1573 K. (b) Phase diagram of the pseudo-binary system Ca_2SiO_4-$Ca_3P_2O_8$.

1 Introduction

The ternary system, calcium oxide-silicon oxide-phosphorus oxide, constitutes one of the most fundamental steelmaking slags. Figure 1(a) gives the iso-thermal section of the ternary system CaO-SiO_2-P_2O_5 near the CaO apex at 1573 K, determined by the present authors /1/. As can be seen in Figure 1(a), this system has the following double oxides;

di-calcium silicate	$Ca_2SiO_4 = 2CaO \cdot SiO_2 = C_2S$
tri-calcium silicate	$Ca_3SiO_5 = 3CaO \cdot SiO_2 = C_3S$
tri-calcium phosphate	$Ca_3P_2O_8 = 3CaO \cdot P_2O_5 = C_3P$
tetra-calcium phosphate	$Ca_4P_2O_9 = 4CaO \cdot P_2O_5 = C_4P$

It has been known that solid solutions form between di-calcium silicate, Ca_2SiO_4, and tri-calcium phosphate, $Ca_3P_2O_8$. Figure 1(b) shows the pseudo-binary phase diagram of Ca_2SiO_4-$Ca_3P_2O_8$ based upon the work of Fix *et al.* /2/ and includes the following triple oxides;

$$Ca_7P_2Si_2O_{16} = 7CaO \cdot P_2O_5 \cdot 2SiO_2 = C_7PS_2$$

$$Ca_5P_2SiO_{12} = 5CaO \cdot P_2O_5 \cdot SiO_2 = C_5PS$$

Figure 1(b) illustrates that the temperatures of the phase transformations from α'-C_2S to α-C_2S and from α-C_3P to $\bar{\alpha}$-C_3P are 1693 K and 1743 K, respectively, and solid solutions $\langle C_2S\text{-}C_3P\rangle ss$ form between α-C_2S and $\bar{\alpha}$-C_3P. As seen in Figure 1(a), $\langle C_2S\text{-}C_3P\rangle ss$ can coexist with solid CaO at 1573 K although the stoichiometric compounds of C_2S and C_3P can not. This is consistent with the observation that, during phosphorus removal from hot metal, phosphorus would often be present in $\langle C_2S\text{-}C_3P\rangle ss$ coexisting with

solid CaO /3/. A better understanding of dephosphorization process would rely on the knowledge of the thermodynamic properties of $\langle C_2S\text{-}C_3P\rangle ss$, whereas there has been a definite lack of such data. The present study is aimed at deriving the activities of the components at 1573 K by applying solution models to $\langle C_2S\text{-}C_3P\rangle ss$.

2 Calculation

2.1 Solution models

Figure 1(b) reported by Fix *et al.* /2/ shows that solid solutions $\langle C_2S\text{-}C_3P\rangle ss$ could form between higher-temperature forms of Ca_2SiO_4 and $Ca_3P_2O_8$, represented by $\alpha\text{-}C_2S$ and $\bar{\alpha}\text{-}C_3P$, respectively. The lattice structures of these solid phases have not been clarified /2/. As illustrated schematically in Figure 2, however, it is not unacceptable that electrically neutral molecules of "$(1/2)Ca_3P_2O_8$" would replace with those of "Ca_2SiO_4", depending on compositions of solid solutions. Such a simple assumption derives the definition of the substitution ratio Y, given as

$$Y \equiv n_{(1/2)Ca_3P_2O_8}/(n_{Ca_2SiO_4} + n_{(1/2)Ca_3P_2O_8}) \tag{1}$$

where n_i denotes the number of moles of component i in solid solutions. The consideration that the molecular mass of "$(1/2)Ca_3P_2O_8$" is half of that of $Ca_3P_2O_8$ leads to equation (2).

$$n_{(1/2)Ca_3P_2O_8} = 2n_{Ca_3P_2O_8} \tag{2}$$

Inserting equation (2) into equation (1), we have

$$Y = 2n_{Ca_3P_2O_8}/(n_{Ca_2SiO_4} + 2n_{Ca_3P_2O_8}) \tag{3}$$

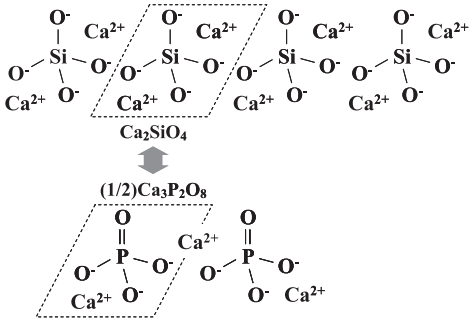

Fig. 2: Schematic illustration of solid solution between Ca_2SiO_4 and $Ca_3P_2O_8$.

The present study is aimed at deriving the relative partial molar Gibbs free energies of Ca_2SiO_4 and $Ca_3P_2O_8$ within $\langle C_2S\text{-}C_3P\rangle ss$ at 1573 K. Towards this objective, the ideal solution model and the regular solution model were applied to solid solutions $\langle C_2S\text{-}C_3P\rangle ss$ between $\alpha\text{-}C_2S$ and $\bar{\alpha}\text{-}C_3P$. The activities of Ca_2SiO_4 and $Ca_3P_2O_8$ referred to the most stable forms at 1573 K as standard states, *i.e.*, $\alpha'\text{-}C_2S$ and $\alpha\text{-}C_3P$, could be formulated as follows.

Ideal Solution Model

$$RT \ln a_{Ca_2SiO_4} = \Delta G°_t(Ca_2SiO_4) + RT \ln(1 - Y) \tag{4}$$

$$RT \ln a_{Ca_3P_2O_8} = 2RT \ln a_{(1/2)Ca_3P_2O_8} = \Delta G°_t(Ca_3P_2O_8) + 2RT \ln Y \tag{5}$$

Regular Solution Model

$$RT \ln a_{Ca_2SiO_4} = \Delta G°_t(Ca_2SiO_4) + RT \ln(1 - Y) + \Omega Y^2 \tag{6}$$

$$RT \ln a_{Ca_3P_2O_8} = 2RT \ln a_{(1/2)Ca_3P_2O_8} = \Delta G°_t(Ca_3P_2O_8) + 2RT \ln Y + 2\Omega(1 - Y)^2 \tag{7}$$

where R is the gas constant, $\Delta G°_t(Ca_2SiO_4)$ and $\Delta G°_t(Ca_3P_2O_8)$ represent the Gibbs free energy changes of the phase transformations of Ca_2SiO_4 and $Ca_3P_2O_8$, respectively, and Ω is the interaction parameter independent of composition and temperature.

2.2 Thermodynamic data used for calculations and necessary conditions

Kubashewski, Alcock and Spencer listed the thermal data on Ca_2SiO_4, *i.e.*, heat capacities of $\alpha'\text{-}C_2S$ and $\alpha\text{-}C_2S$, and heat of the phase transformation /4/. By extrapolating the data for heat capacity of $\alpha\text{-}C_2S$ at temperature below 1693 K, the value for $\Delta G°_t(Ca_2SiO_4)$ at 1573 K could be calculated as

$$\Delta G°_t(Ca_2SiO_4) \equiv G°(\alpha\text{-}C_2S) - G°(\alpha'\text{-}C_2S) = 1{,}132\ \mathrm{J \cdot mol^{-1}} \quad \text{at 1573 K} \tag{8}$$

where $G°(i)$ is the standard Gibbs free energy of substance i. On the other hand, the literature data have been lacking for the calculation of $\Delta G°_t(Ca_3P_2O_8)$. Therefore, the following formula was assumed in this study.

$$\Delta G°_t(Ca_3P_2O_8) \equiv G°(\bar{\alpha}\text{-}C_3P) - G°(\alpha\text{-}C_3P) = \Delta H°_t(Ca_3P_2O_8)\,(1 - T/1743) \tag{9}$$

where $\Delta H°_t(Ca_3P_2O_8)$ is the heat of the phase transportation from $\alpha\text{-}C_3P$ to $\bar{\alpha}\text{-}C_3P$ at the transition temperature of 1743 K.

The reactions of the formations of Ca_2SiO_4 and Ca_3SiO_5 from CaO and SiO_2 are expressed as

$$2\,CaO + SiO_2 = Ca_2SiO_4 \quad (10)$$

$$3\,CaO + SiO_2 = Ca_3SiO_5 \quad (11)$$

The present authors assessed the thermal data by Kubaschewski *et al.* /4/ to derive the equilibrium constants of reactions (10) and (11) thermodynamically consistent with phase diagrams; the results could be given as follows /5/.

$$\log K(10) = \log a_{Ca_2SiO_4} - 2\log a_{CaO} - \log a_{SiO_2} = 4.78 \quad \text{at 1573 K} \quad (12)$$

$$\log K(11) = \log a_{Ca_3SiO_5} - 3\log a_{CaO} - \log a_{SiO_2} = 4.80 \quad \text{at 1573 K} \quad (13)$$

where a_i represents the activities of substance i referred to pure i of the most stable form at 1573 K. For the standard Gibbs free energy changes of the formations of $Ca_3P_2O_8$ and $Ca_4P_2O_9$ from CaO and P_2O_5, the following literature data were accepted.

$$3\,CaO + P_2O_5 = Ca_3P_2O_8 \quad (14)$$

$$\Delta G(14)^\circ = -RT\ln K(14) = -776{,}300 + 18.6 \times (T/\mathrm{K})\ (\mathrm{J\cdot mol^{-1}}) \quad /6, 7/ \quad (15)$$

$$\log K(14) = \log a_{Ca_3P_2O_8} - 3\log a_{CaO} - \log a_{P_2O_5} = 24.80 \quad \text{at 1573 K} \quad (16)$$

$$4\,CaO + P_2O_5 = Ca_4P_2O_9 \quad (17)$$

$$\Delta G(17)^\circ = -RT\ln K(17) = -781{,}500 + 14.8 \times (T/\mathrm{K})\ (\mathrm{J\cdot mol^{-1}}) \quad /7/ \quad (18)$$

$$\log K(17) = \log a_{Ca_4P_2O_9} - 4\log a_{CaO} - \log a_{P_2O_5} = 25.18 \quad \text{at 1573 K} \quad (19)$$

In this study, $a_{P_2O_5}$ represents the activity of P_2O_5 referred to hypothetical pure liquid P_2O_5 /8/.

As shown in Figure 1(a), the iso-thermal section of the $CaO\text{-}SiO_2\text{-}P_2O_5$ system near the CaO apex at 1573 K consists of the following three-phase assemblages.

$\langle C_2S\text{-}C_3P\rangle ss + Ca_2SiO_4 + Ca_3SiO_5$; triangle b-a-Ca_3SiO_5

$\langle C_2S\text{-}C_3P\rangle ss + CaO + Ca_3SiO_5$; triangle c-CaO-Ca_3SiO_5

$\langle C_2S\text{-}C_3P\rangle ss + CaO + Ca_7P_2Si_2O_{16}$; triangle d-CaO-e

$\langle C_2S\text{-}C_3P\rangle ss + CaO + Ca_7P_2Si_2O_{16}$; triangle g-CaO-f

$\langle C_2S\text{-}C_3P\rangle ss + CaO + Ca_5P_2SiO_{12}$; triangle h-CaO-i

$CaO + Ca_4P_2O_9 + Ca_5P_2SiO_{12}$; triangle CaO-$Ca_4P_2O_9$-$j$

$\langle C_2S\text{-}C_3P\rangle ss + Ca_4P_2O_9 + Ca_5P_2SiO_{12}$; triangle l-$Ca_4P_2O_9$-k

$\langle C_2S\text{-}C_3P\rangle ss + Ca_4P_2O_9 + Ca_3P_2O_8$; triangle m-$Ca_4P_2O_9$-n

It should be noticed here that the compounds of Ca_2SiO_4, $Ca_7P_2Si_2O_{16}$, $Ca_5P_2SiO_{12}$ and $Ca_3P_2O_8$ included in these three-phase regions were non-stoichiometric. The compositions of points a, b, d, e, f, g, h, i, k, l, m and n could be read off by using the scales of the mole fractions of SiO_2 and P_2O_5 in Figure 1(a), while those of points c and j have not been determined precisely /1/. Table 1 summarizes the values for Y in $\langle C_2S\text{-}C_3P\rangle ss$ at compositions b, h, l and m. Based on

Region	Y in $\langle C_2S\text{-}C_3P\rangle ss$	$a_{Ca_2SiO_4}$	$a_{Ca_3P_2O_8}$	log a_{CaO}	log a_{SiO_2}	log $a_{P_2O_5}$	Remark
$\langle C_2S\text{-}C_3P\rangle ss + Ca_2SiO_4 + Ca_3SiO_5$ (triangle b-a-Ca_3SiO_5)	0.088	0.995[a]	0.016	−0.02	−4.75	−26.53[a]	log $a_{P_2O_5} = -26.53$; Eq. (28) $a_{Ca_2SiO_4} < 1$; Eq. (20)
$\langle C_2S\text{-}C_3P\rangle ss + CaO + Ca_5P_2SiO_{12}$ (triangle h-CaO-i)	0.592	0.445	0.745[b]	0.00	−5.13	−24.93	$a_{Ca_3P_2O_8} < 0.417$; Eq. (25)
$\langle C_2S\text{-}C_3P\rangle ss + Ca_4P_2O_9 + Ca_5P_2SiO_{12}$ (triangle l-$Ca_4P_2O_9$-k)	0.748	0.274	1.193[b]	−0.46	−4.43	−23.35	$0.417 < a_{Ca_3P_2O_8} < 1$; Eq. (26)
$\langle C_2S\text{-}C_3P\rangle ss + Ca_4P_2O_9 + Ca_3P_2O_8$ (triangle m-$Ca_4P_2O_9$-n)	0.841	0.173	1.507[b]	−0.56	−4.33	−22.95	$a_{Ca_3P_2O_8} < 1$; Eq. (21)

a) The values with superscript "a" satisfied the necessary conditions.
b) The values with superscript "b" did not satisfy the necessary conditions.

Table 1: Calculation results of the ideal solution model with $\Delta H^\circ_t(Ca_3P_2O_8) = 101\ \mathrm{kJ\cdot mol^{-1}}$.

the thermodynamic considerations of the phase relations, the conditions which the solution models should satisfy were mentioned below.

As seen in Figure 1(b), $Ca_3P_2O_8$ is soluble in α'-C_2S; point *a* represents the solubility limit at 1573 K. Such a solubility requires that the Ca_2SiO_4 activity at point *a* is to be less than unity. According to the Condenced Phase Rule, when three phases coexist in a three-component system, there is only one degree of freedom. This implies that for a particular temperature, there are zero degrees of freedom; the Ca_2SiO_4 activity is independent of the bulk composition in the three-phase region of $\langle C_2S\text{-}C_3P\rangle ss + Ca_2SiO_4 + Ca_3SiO_5$ (triangle *b*-*a*-Ca_3SiO_5). Namely, the Ca_2SiO_4 activity within $\langle C_2S\text{-}C_3P\rangle ss$ at point *b* is equivalent to that at point *a* and hence to be less than unity.

$$a_{Ca_2SiO_4} < 1 \quad \text{(at point } b\text{; } Y = 0.088,\ T = 1573\ \text{K)} \qquad (20)$$

In analogy with this, for the three-phase region of $\langle C_2S\text{-}C_3P\rangle ss + Ca_4P_2O_9 + Ca_3P_2O_8$ (triangle *m*-$Ca_4P_2O_9$-*n*), the solubility of Ca_2SiO_4 in α-C_3P requires that the $Ca_3P_2O_8$ activity within $\langle C_2S\text{-}C_3P\rangle ss$ at composition *m* is less than unity.

$$a_{Ca_3P_2O_8} < 1 \quad \text{(at point } m\text{; } Y = 0.841,\ T = 1573\ \text{K)} \qquad (21)$$

The P_2O_5 activity within the three-phase assemblage of $CaO + Ca_4P_2O_9 + Ca_5P_2SiO_{12}$ (triangle CaO-$Ca_4P_2O_9$-*j*) can be calculated from equation (19) with the unit activities of CaO and $Ca_4P_2O_9$.

$$\log a_{P_2O_5} = -\log K(17) = -25.18 \quad \text{at 1573 K} \qquad (22)$$

Inserting equation (22) into equation (16), the activity of hypothetical solid $Ca_3P_2O_8$ in the three-phase region of $CaO + Ca_4P_2O_9 + Ca_5P_2SiO_{12}$ can be evaluated as

$$\log a_{Ca_3P_2O_8} = \log K(14) - \log K(17) = -0.38 \quad \text{at 1573 K} \qquad (23)$$

$$a_{Ca_3P_2O_8} = 0.417 \quad \text{at 1573 K} \qquad (24)$$

Along the Ca_2SiO_4-$Ca_3P_2O_8$ edge in Figure 1(a), the $Ca_3P_2O_8$ activity should increase with an increase in the $Ca_3P_2O_8$ concentration. Therefore, the $Ca_3P_2O_8$ activity in the three-phase region of $CaO + Ca_4P_2O_9 + Ca_5P_2SiO_{12}$ is to be greater than that at point *h* and is to be smaller than that at point *l*. Thus, we obtain the following inequalities.

$$a_{Ca_3P_2O_8} < 0.417 \quad \text{(at point } h\text{; } Y = 0.592,\ T = 1573\ \text{K)} \qquad (25)$$

$$0.417 < a_{Ca_3P_2O_8} < 1 \quad \text{(at point } l\text{; } Y = 0.748,\ T = 1573\ \text{K)} \qquad (26)$$

The P_2O_5 activity in $\langle C_2S\text{-}C_3P\rangle ss$ at composition *b* was determined by the present authors through a gas equilibrium method /9/. Molten copper containing phosphorus was brought to equilibrium with mixtures of $\langle C_2S\text{-}C_3P\rangle ss + Ca_2SiO_4 + Ca_3SiO_5$ in a stream of $Ar + H_2 + H_2O$ gas mixtures. The results were expressed as

$$RT \ln a_{P_2O_5} = -1{,}106{,}000 + 194.7 \times (T/\text{K}) \quad (\text{J} \cdot \text{mol}^{-1}) \qquad (27)$$

$$\log a_{P_2O_5} = -26.53 \quad \text{(at point } b,\ T = 1573\ \text{K)} \qquad (28)$$

On the other hand, by using equations (12), (13) and (16) with the unit activity of Ca_3SiO_5, $a_{P_2O_5}$ in the three-phase region of $\langle C_2S\text{-}C_3P\rangle ss + Ca_2SiO_4 + Ca_3SiO_5$ can be expressed as

$$\begin{aligned}\log a_{P_2O_5} &= 3 \log a_{Ca_2SiO_4} + \log a_{Ca_3P_2O_8} - 3 \log K(10) \\ &\quad + 3 \log K(11) - \log K(14) \\ &= 3 \log a_{Ca_2SiO_4} + \log a_{Ca_3P_2O_8} \\ &\quad - 24.74 \quad \text{(at 1573 K)}\end{aligned} \qquad (29)$$

Combining equations (28) and (29), we have

$$\begin{aligned}&3 \log a_{Ca_2SiO_4} + \log a_{Ca_3P_2O_8} = -1.79 \\ &\text{(at point } b\text{; } Y = 0.088,\ T = 1573\ \text{K)}\end{aligned} \qquad (30)$$

Equation (30) should hold when the values for $a_{Ca_2SiO_4}$ and $a_{Ca_3P_2O_8}$ at composition *b* evaluated with the solution models are inserted.

3 Calculation results

When the ideal solution model was applied to solid solutions $\langle C_2S\text{-}C_3P\rangle ss$, combining equations (4), (5), (8) and (9) gave the following formulae for the activities of Ca_2SiO_4 and $Ca_3P_2O_8$ at 1573 K.

$$\log a_{Ca_2SiO_4} = 3.76 \times 10^{-2} + \log(1 - Y) \qquad (31)$$

$$\begin{aligned}\log a_{Ca_3P_2O_8} &= 2 \log a_{(1/2)Ca_3P_2O_8} \\ &= 3.24 \times 10^{-6} \times \Delta H^\circ_t(Ca_3P_2O_8) + 2 \log Y\end{aligned} \qquad (32)$$

The ideal solution model used in this study had one undetermined parameter, *viz.*, $\Delta H^\circ_t(Ca_3P_2O_8)$. Inserting equations (31) and (32) into equation (30), the value for $\Delta H^\circ_t(Ca_3P_2O_8)$ could be determined as

$$\Delta H^\circ_t(Ca_3P_2O_8)/\text{J} \cdot \text{mol}^{-1} = 1.01 \times 10^5 \qquad (33)$$

Thus, the activities of $Ca_3P_2O_8$ at 1573 K could be expressed as

$$\log a_{Ca_3P_2O_8} = 2 \log a_{(1/2)Ca_3P_2O_8} = 3.28 \times 10^{-1} + 2 \log Y \quad (34)$$

Rewriting equations (31) and (34), we had

$$a_{Ca_2SiO_4} = 1.09 \times (1 - Y) \quad (35)$$

$$a_{(1/2)Ca_3P_2O_8} = 1.46 \times Y \quad (36)$$

$$a_{Ca_3P_2O_8} = (a_{(1/2)Ca_3P_2O_8})^2 = (1.46 \times Y)^2 \quad (37)$$

The numbers of 1.09 in equation (35) and 1.46 in equation (36), respectively, indicated the activities of α-Ca_2SiO_4 with reference to α′-Ca_2SiO_4 as the standard state and that of $\bar{\alpha}$-"(1/2)$Ca_3P_2O_8$" with reference to α-"(1/2)$Ca_3P_2O_8$" as the standard state at 1573 K. Dotted lines in Figure 3(b) shows $a_{Ca_2SiO_4}$ and $a_{(1/2)Ca_3P_2O_8}$ at 1573 K based on equations (35) and (36). As seen in this figure, $a_{Ca_2SiO_4}$ and $a_{(1/2)Ca_3P_2O_8}$ within $\langle C_2S\text{-}C_3P\rangle ss$ were proportional to $(1 - Y)$ and Y, respectively. Figure 3(a) is the redrawn pseudo-binary phase diagram of Ca_2SiO_4-$Ca_3P_2O_8$, in which compositions are shown by the values for Y. According to the Condensed Phase Rule, the activities were constant within the two-phase regions of *a*-*b*, *d*-*e*, *f*-*g*, *h*-*i*, *k*-*l* and *m*-*n*. The values for $a_{Ca_3P_2O_8}$ were obtainable from equation (37) and could be read off by using the subsidiary scale added to Figure 3(b). Table 1 summarizes $a_{Ca_2SiO_4}$ and $a_{Ca_3P_2O_8}$ at compositions *b*, *h*, *l* and *m*. As seen in Table 1, the values for $a_{Ca_3P_2O_8}$ at points *h*, *l* and *m* did not satisfy inequalities (25), (26) and (21), respectively. These results led to the conclusion that the ideal solution model could not give the relative partial molar Gibbs free energies of the components within $\langle C_2S\text{-}C_3P\rangle ss$.

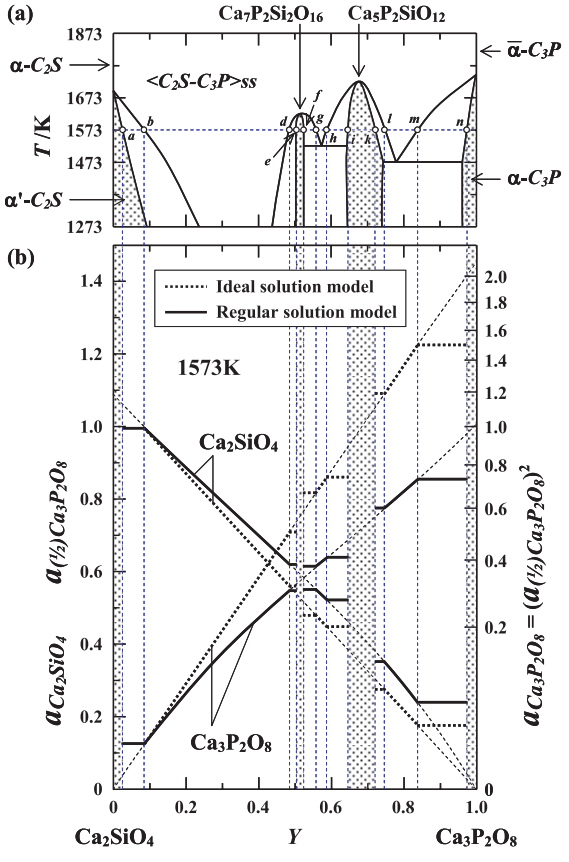

Fig. 3: (a) Phase diagram of the pseudo-binary system Ca_2SiO_4-$Ca_3P_2O_8$. (b) Activities of Ca_2SiO_4 and $Ca_3P_2O_8$ as functions of the substitution ratio Y.

On the other hand, the regular solution model gave the following equations by combining equations (6), (7), (8) and (9).

$$\log a_{Ca_2SiO_4} = 3.76 \times 10^{-2} + \log(1 - Y) + 3.32 \times 10^{-5} \times \Omega Y^2 \quad (38)$$

$$\log a_{Ca_3P_2O_8} = 2 \log a_{(1/2)Ca_3P_2O_8} = 3.24 \times 10^{-6} \times \Delta H°_t(Ca_3P_2O_8) + 2 \log Y + 6.64 \times 10^{-5} \times \Omega(1 - Y)^2 \quad (39)$$

These formulae included undetermined parameters, *viz.*, $\Delta H°_t(Ca_3P_2O_8)$ and Ω. Inserting equations (38) and (39) into equation (30), the relation between $\Delta H°_t(Ca_3P_2O_8)$ and Ω was obtained as

$$\Omega = 5.86 \times 10^3 - 5.79 \times 10^{-2} \times \Delta H°_t(Ca_3P_2O_8) \quad (40)$$

Substituting equation (40) into equations (38) and (39), the activities of Ca_2SiO_4 and $Ca_3P_2O_8$ could be expressed as functions of $\Delta H°_t(Ca_3P_2O_8)$ and Y.

$$\log a_{Ca_2SiO_4} = 3.76 \times 10^{-2} + \log(1 - Y) + [1.95 \times 10^{-1} - 1.92 \times 10^{-6} \times \Delta H°_t(Ca_3P_2O_8)] \times Y^2 \quad (41)$$

$$\log a_{Ca_3P_2O_8} = 2 \log a_{(1/2)Ca_3P_2O_8} = 3.24 \times 10^{-6} \times \Delta H°_t(Ca_3P_2O_8) + 2 \log Y + [3.90 \times 10^{-1} - 3.84 \times 10^{-6} \times \Delta H°_t(Ca_3P_2O_8)] \times (1 - Y)^2 \quad (42)$$

Under the conditions that the values calculated from equations (41) and (42) satisfied inequalities (20), (21), (25) and (26), $\Delta H°_t(Ca_3P_2O_8)$ was determined as

$$\Delta H°_t(Ca_3P_2O_8)/\mathrm{J \cdot mol^{-1}} = (2.10 \pm 2.10) \times 10^3 \quad (43)$$

Inserting equation (43) to equation (40), we had

$$\Omega/\mathrm{J \cdot mol^{-1}} = (5.74 \pm 0.12) \times 10^3 \quad (44)$$

Combining equations (38), (39), (43) and (44), the activities of Ca_2SiO_4 and $Ca_3P_2O_8$ at 1573 K were expressed as

Region	Y in $\langle C_2S\text{-}C_3P\rangle ss$	$a_{Ca_2SiO_4}$	$a_{Ca_3P_2O_8}$	log a_{CaO}	log a_{SiO_2}	log $a_{P_2O_5}$	Remark
$\langle C_2S\text{-}C_3P\rangle ss + Ca_2SiO_4 + Ca_3SiO_5$ (triangle b-a-Ca_3SiO_5)	0.088	0.998[a] ± 0.000	0.016 ± 0.000	−0.02 ± 0.00	−4.74 ± 0.00	−26.53[a]	log $a_{P_2O_5} = -26.53$; Eq. (28) $a_{Ca_2SiO_4} < 1$; Eq. (20)
$\langle C_2S\text{-}C_3P\rangle ss + CaO + Ca_3SiO_5$ (triangle c-CaO-Ca_3SiO_5)	0.131 ± 0.000	0.955 ± 0.000	0.034 ± 0.000	0.00	−4.80	−26.27 ± 0.00	–
$\langle C_2S\text{-}C_3P\rangle ss + CaO + Ca_7P_2Si_2O_{16}$ (triangle d-CaO-e)	0.493	0.615 ± 0.001	0.309 ± 0.003	0.00	−4.99 ± 0.00	−25.31 ± 0.00	–
$\langle C_2S\text{-}C_3P\rangle ss + CaO + Ca_7P_2Si_2O_{16}$ (triangle g-CaO-f)	0.560	0.550 ± 0.001	0.378 ± 0.005	0.00	−5.04 ± 0.00	−25.22 ± 0.01	–
$\langle C_2S\text{-}C_3P\rangle ss + CaO + Ca_5P_2SiO_{12}$ (triangle h-CaO-i)	0.592	0.519 ± 0.001	0.412[a] ± 0.005	0.00	−5.06 ± 0.01	−25.19 ± 0.01	$a_{Ca_3P_2O_8} < 0.417$; Eq. (25)
$\langle C_2S\text{-}C_3P\rangle ss + Ca_4P_2O_9 + Ca_5P_2SiO_{12}$ (triangle l-$Ca_4P_2O_9$-k)	0.748	0.351 ± 0.002	0.602[a] ± 0.008	−0.16 ± 0.01	−4.92 ± 0.01	−24.54 ± 0.02	$0.417 < a_{Ca_3P_2O_8} < 1$; Eq. (26)
$\langle C_2S\text{-}C_3P\rangle ss + Ca_4P_2O_9 + Ca_3P_2O_8$ (triangle m-$Ca_4P_2O_9$-n)	0.841	0.236 ± 0.001	0.735[a] ± 0.011	−0.25 ± 0.01	−4.91 ± 0.01	−24.19 ± 0.02	$a_{Ca_3P_2O_8} < 1$; Eq. (21)

a) The values with superscript "a" satisfied the necessary conditions.

Table 2: Calculation results of the regular solution model with $\Delta H°_t(Ca_3P_2O_8) = 2.10 \pm 2.10$ kJ · mol^{-1} and $\Omega = 5.74 \pm 0.12$ kJ · mol^{-1}.

$$\log a_{Ca_2SiO_4} = 3.76 \times 10^{-2} + \log(1 - Y) + 1.91 \times 10^{-1} \times Y^2 \quad (45)$$

$$\log a_{Ca_3P_2O_8} = 2 \log a_{(1/2)Ca_3P_2O_8} = 6.80 \times 10^{-3} + 2 \log Y + 3.81 \times 10^{-1} \times (1 - Y)^2 \quad (46)$$

Table 2 gives the present values for $a_{Ca_2SiO_4}$ and $a_{Ca_3P_2O_8}$ calculated from equations (45) and (46). The uncertainties of the activities in Table 2 were based on the inaccuracies of $\Delta H°_t(Ca_3P_2O_8)$ and Ω given in equations (43) and (44). As seen in this table, inequalities (20), (25), (26) and (21) held with the present results at compositions b, h, l and m, respectively. Solid curves in Figure 3(b) represent the activity-composition curves evaluated from equations (45) and (46). These curves were slightly convex upward owing to the positive value for the interaction parameter Ω. As already mentioned above, the activities were constant in the two-phase regions. For example, the $Ca_3P_2O_8$ activity at point h was equal to that at point i. The hatched areas in Figure 3 denote the composition ranges of non-stoichiometric compounds of α'-Ca_2SiO_4, $Ca_7P_2Si_2O_{16}$, $Ca_5P_2SiO_{12}$ and α-$Ca_3P_2O_8$, in which activity-composition curves could not be obtained in this study.

4 Discussion

Figure 4(a) shows the iso-thermal section of the ternary system CaO-SiO_2-P_2O_5 near the CaO apex at 1573 K; this figure is identical to Figure 1(a). By using the present results of the regular solution model, the activities of CaO, SiO_2 and P_2O_5 could be calculated within the following regions.

$\langle C_2S\text{-}C_3P\rangle ss + Ca_2SiO_4 + Ca_3SiO_5$; triangle b-a-Ca_3SiO_5

$\langle C_2S\text{-}C_3P\rangle ss + Ca_3SiO_5$; region b-c-Ca_3SiO_5

$\langle C_2S\text{-}C_3P\rangle ss + CaO + Ca_3SiO_5$; triangle c-CaO-Ca_3SiO_5

$\langle C_2S\text{-}C_3P\rangle ss + CaO$; region c-d-CaO

$\langle C_2S\text{-}C_3P\rangle ss + CaO + Ca_7P_2Si_2O_{16}$; triangle d-CaO-e

$\langle C_2S\text{-}C_3P\rangle ss + CaO + Ca_7P_2Si_2O_{16}$; triangle g-CaO-f

$\langle C_2S\text{-}C_3P\rangle ss + CaO$; region g-h-CaO

$\langle C_2S\text{-}C_3P\rangle ss + CaO + Ca_5P_2SiO_{12}$; triangle h-CaO-i

$\langle C_2S\text{-}C_3P\rangle ss + Ca_4P_2O_9 + Ca_5P_2SiO_{12}$; triangle l-$Ca_4P_2O_9$-k

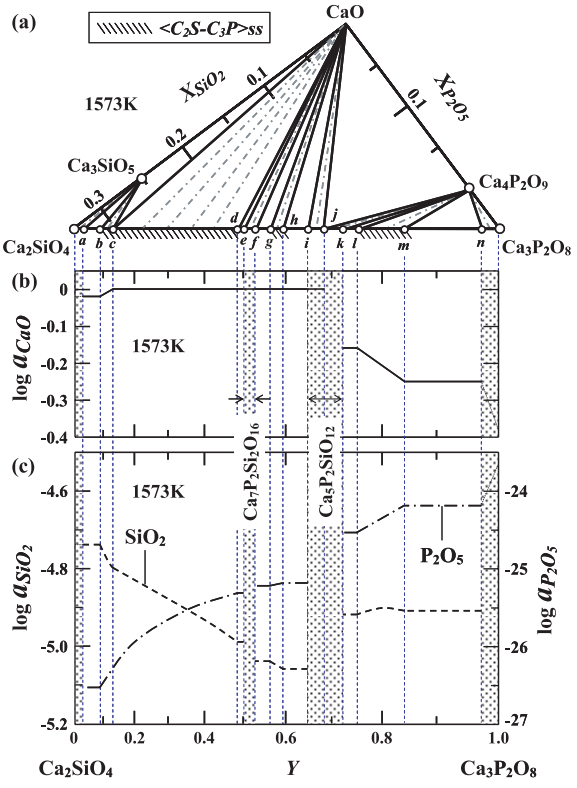

Fig. 4: (a) Iso-thermal section of the ternary system CaO-SiO_2-P_2O_5 near the CaO apex at 1573 K. (b) Activities of CaO at 1573 K. (c) Activities of SiO_2 and P_2O_5 at 1573 K.

$$\langle C_2S\text{-}C_3P\rangle ss + Ca_4P_2O_9\text{; region } l\text{-}m\text{-}Ca_4P_2O_9$$

$$\langle C_2S\text{-}C_3P\rangle ss + Ca_4P_2O_9 + Ca_3P_2O_8\text{; triangle } m\text{-}Ca_4P_2O_9\text{-}n$$

Such regions could be classified by solid phases coexisting with $\langle C_2S\text{-}C_3P\rangle ss$, *viz.*, Ca_3SiO_5, CaO and $Ca_4P_2O_9$.

In the regions including Ca_3SiO_5, the activity of Ca_3SiO_5 should be unity. Therefore, equation (13) could be rewritten as

$$\log K(11) = -3 \log a_{CaO} - \log a_{SiO_2} \quad (47)$$

Solving simultaneous equations (12), (16) and (47), we had

$$\log a_{CaO} = -\log a_{Ca_2SiO_4} + \log K(10) - \log K(11) \quad (48)$$

$$\log a_{SiO_2} = 3 \log a_{Ca_2SiO_4} - 3 \log K(10) + 2 \log K(11) \quad (49)$$

$$\log a_{P_2O_5} = \log a_{Ca_3P_2O_8} + 3 \log a_{Ca_2SiO_4} - 3 \log K(10) + 3 \log K(11) - \log K(14) \quad (50)$$

Combining equations (45), (46), (48), (49) and (50), the activities of CaO, SiO_2 and P_2O_5 at 1573 K in the two-phase region of $\langle C_2S\text{-}C_3P\rangle ss + Ca_3SiO_5$ (region *b*-*c*-Ca_3SiO_5) could be expressed as the functions of *Y*.

$$\log a_{CaO} = -0.06 - \log(1 - Y) - 1.91 \times 10^{-1} \times Y^2 \quad (51)$$

$$\log a_{SiO_2} = -4.63 + 3 \log(1 - Y) + 5.73 \times 10^{-1} \times Y^2 \quad (52)$$

$$\log a_{P_2O_5} = -24.62 + 3 \log(1 - Y) + 2 \log Y + 5.73 \times 10^{-1} \times Y^2 + 3.81 \times 10^{-1} \times (1 - Y)^2 \quad (53)$$

The activities in the three-phase region of $\langle C_2S\text{-}C_3P\rangle ss + Ca_2SiO_4 + Ca_3SiO_5$ (triangle *b*-*a*-Ca_3SiO_5) could be calculated by inserting $Y = 0.088$ at point *b* into equations (51), (52) and (53).

$$\log a_{CaO} = -0.02 \quad \text{(at point } b\text{; } Y = 0.088, T = 1573 \text{ K)} \quad (54)$$

$$\log a_{SiO_2} = -4.74 \quad \text{(at point } b\text{; } Y = 0.088, T = 1573 \text{ K)} \quad (55)$$

$$\log a_{P_2O_5} = -26.53 \quad \text{(at point } b\text{; } Y = 0.088, T = 1573 \text{ K)} \quad (56)$$

On the other hand, the composition of $\langle C_2S\text{-}C_3P\rangle ss$ in equilibrium with Ca_3SiO_5 and CaO, *i.e.*, point *c*, has not been reported. By solving equation (51) under the condition that $\log a_{CaO} = 0$, this composition could be estimated as

$$Y = 0.131 \quad \text{(at point } c, T = 1573 \text{ K)} \quad (57)$$

Inserting equation (57) to equations (52) and (53), the SiO_2 and P_2O_5 activities in the three-phase assemblage of $\langle C_2S\text{-}C_3P\rangle ss + CaO + Ca_3SiO_5$ (triangle *c*-CaO-Ca_3SiO_5) were obtained as

$$\log a_{SiO_2} = -4.80 \quad \text{(at point } c\text{; } Y = 0.131, T = 1573 \text{ K)} \quad (58)$$

$$\log a_{P_2O_5} = -26.27 \quad \text{(at point } c\text{; } Y = 0.131, T = 1573 \text{ K)} \quad (59)$$

The CaO activity in the regions including CaO should be unity. Thus, equations (12) and (16), respectively, could be rewritten as

$$\log a_{SiO_2} = \log a_{Ca_2SiO_4} - \log K(10) \quad (60)$$

$$\log a_{P_2O_5} = \log a_{Ca_3P_2O_8} - \log K(14) \quad (61)$$

Combining equations (45), (46), (60) and (61), the SiO_2 and P_2O_5 activities within the two-phase resion of $\langle C_2S\text{-}C_3P\rangle ss + CaO$ (regions *c*-*d*-CaO and *g*-*h*-CaO) were given as

$$\log a_{SiO_2} = -4.74 + \log(1 - Y) + 1.91 \times 10^{-1} \times Y^2 \quad (62)$$

$$\log a_{P_2O_5} = -24.79 + 2 \log Y + 3.81 \times 10^{-1} \times (1 - Y)^2 \quad (63)$$

The values for a_{SiO_2} and $a_{P_2O_5}$ in the three-phase regions of $\langle C_2S\text{-}C_3P\rangle ss + CaO + Ca_7P_2Si_2O_{16}$ (triangles *d*-CaO-*e* and *g*-CaO-*f*) and $\langle C_2S\text{-}C_3P\rangle ss + CaO + Ca_5P_2SiO_{12}$ (triangle *h*-CaO-*i*) could be calculated from equations (62) and (63).

Based on the unit $Ca_4P_2O_9$ activity in the regions including $Ca_4P_2O_9$, equation (19) was rewritten as

$$\log K(17) = -4 \log a_{CaO} - \log a_{P_2O_5} \quad (64)$$

Solving simultaneous equations (12), (16) and (64), we had

$$\log a_{CaO} = -\log a_{Ca_3P_2O_8} + \log K(14) - \log K(17) \quad (65)$$

$$\log a_{SiO_2} = \log a_{Ca_2SiO_4} + 2 \log a_{Ca_3P_2O_8} - \log K(10) - 2 \log K(14) + 2 \log K(17) \quad (66)$$

$$\log a_{P_2O_5} = 4 \log a_{Ca_3P_2O_8} - 4 \log K(14) + 3 \log K(17) \quad (67)$$

Combining equations (45), (46), (65), (66) and (67), the activities at 1573 K in the two-phase region of $\langle C_2S\text{-}C_3P\rangle ss$ + $Ca_4P_2O_9$ (region l-m-$Ca_4P_2O_9$) could be expressed as

$$\log a_{CaO} = -0.39 - 2 \log Y - 3.81 \times 10^{-1} \times (1 - Y)^2 \quad (68)$$

$$\log a_{SiO_2} = -3.97 + \log(1 - Y) + 4 \log Y + 1.91 \times 10^{-1} \times Y^2 + 7.62 \times 10^{-1} \times (1 - Y)^2 \quad (69)$$

$$\log a_{P_2O_5} = -23.63 + 8 \log Y + 1.52 \times (1 - Y)^2 \quad (70)$$

The values for the activities in the three-phase regions of $\langle C_2S\text{-}C_3P\rangle ss + Ca_4P_2O_9 + Ca_5P_2SiO_{12}$ (triangle l-$Ca_4P_2O_9$-k) and $\langle C_2S\text{-}C_3P\rangle ss + Ca_4P_2O_9 + Ca_3P_2O_8$ (triangle m-$Ca_4P_2O_9$-n) could be calculated from equations (68), (69) and (70).

The CaO, SiO_2 and P_2O_5 activities estimated in this study are summarized in Table 2, and illustrated in Figures 4(b) and 4(c). The uncertainties of the values in Table 2 were due to the inaccuracies of $\Delta H°_t(Ca_3P_2O_8)$ and Ω determined in this study. Figure 4(b) shows that the CaO activities are unity between point c and point j; in this composition range, the two- and three-phase regions include solid CaO as seen in Figure 4(a). Figure 4(c) illustrates that the P_2O_5 activities increase monotonically with an increase in the values for Y in $\langle C_2S\text{-}C_3P\rangle ss$. It would be worth mentioning here that the P_2O_5 activity in the two-phase assemblage of stoichiometric $Ca_3P_2O_8$ + $Ca_4P_2O_9$ at 1573 K can be calculated as

$$\log a_{P_2O_5} = -4 \log K(14) + 3 \log K(17) = -23.66 \quad \text{at 1573 K} \quad (71)$$

This value corresponds to the logarithmic activity of P_2O_5 at $Y = 1.0$ in Figure 4(c), and would not be imcompatible with the activity-composition curves determined in this study. On the other hand, the SiO_2 activities do not decrease monotonically with an increase in Y. Magnitude correlations of activities strongly depend on phase relations. Therefore, the behaviour of the SiO_2 and P_2O_5 activities will be able to be explained by future work on the SiO_2-rich and/or P_2O_5-rich areas of the CaO-SiO_2-P_2O_5 ternary iso-thermal section. The present values for $a_{P_2O_5}$ and a_{SiO_2} can be recommended at least as tentative estimates for understanding dephosphorization process.

The reaction of phosphorus removal from molten iron can be represented as

$$2\,[P]_{Fe} + 5\,(FeO)_{slag} = (P_2O_5)_{slag} + 5\,\{Fe\} \quad (72)$$

where $[P]_{Fe}$ is phosphorus in liquid iron, $(FeO)_{slag}$ and $(P_2O_5)_{slag}$ are FeO and P_2O_5 in liquid slag, and {Fe} is liquid iron. For reaction (72), Turkdogan and Pearson derived the following expression /10/.

$$\log K(72) = \log \{a_{P_2O_5}/h_P^2\, a_{FeO}^5\} = -17.7 + 8{,}490/(T/\mathrm{K}) \quad (73)$$

By rewriting equation (73), we have

$$\log h_P = -(1/2) \log K(72) + (1/2) \log a_{P_2O_5} - (5/2) \log a_{FeO} \quad (74)$$

For carbon-saturated {Fe-C-P} liquid alloys, the Henrian activity of phosphorus is given by

$$\log h_P = \log[\%P] + e_P^C\,[\%C] \quad (75)$$

By combining equations (74) and (75), we have

$$\log[\%P] = -e_P^C\,[\%C] - (1/2) \log K(72) + (1/2) \log a_{P_2O_5} - (5/2) \log a_{FeO} = -e_P^C\,[\%C] + (1/2) \log a_{P_2O_5} - (5/2) \log a_{FeO} + 8.9 - 4{,}250/(T/\mathrm{K}) \quad (76)$$

Equation (76) means that the equilibrium phosphorus concentrations can be estimated by using the values for the activities of P_2O_5 and FeO. Figure 5 shows a schematic illustration of the iso-thermal tetrahedron of the pseudo-quaternary system CaO-Ca_2SiO_4-$Ca_3P_2O_8$-FeO at 1573 K, showing the following four-phase assemblages /11/.

$Ca_3SiO_5 + Ca_2SiO_4 + \langle C_2S\text{-}C_3P\rangle ss$ + Liquid; tetrahedron
Ca_3SiO_5-a-b-$L(1)$

CaO + $Ca_3SiO_5 + \langle C_2S\text{-}C_3P\rangle ss$ + Liquid; tetrahedron
CaO-Ca_3SiO_5-c-$L(2)$

CaO + $Ca_4P_2O_9 + Ca_5P_2SiO_{12}$ + Liquid; tetrahedron
CaO-$Ca_4P_2O_9$-j-$L(3)$

According to the Condensed Phase Rule, when four phases coexist in a four-component system, there is only one

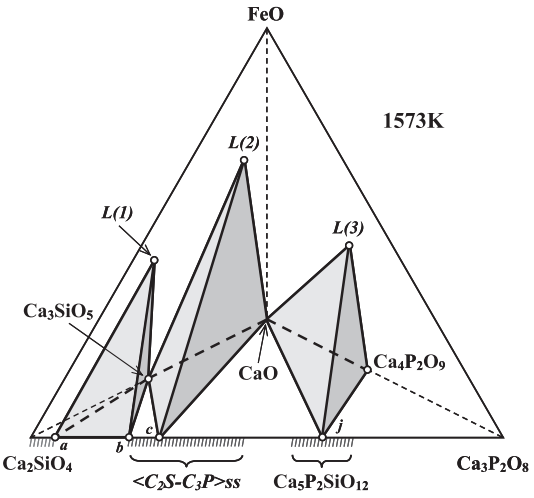

Fig. 5: Schematic illustration of the iso-thermal tetrahedron showing the phase relations in the pseudo-quaternary system CaO-Ca_2SiO_4-$Ca_3P_2O_9$-FeO coexisitng with metallic iron at 1573 K.

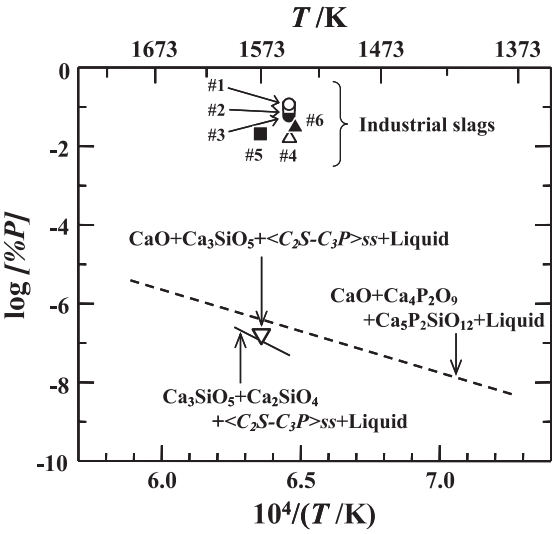

Fig. 6: Estimated phosphorus contents in molten iron.

degree of freedom. This implies that for a particular temperature, the activities of FeO and P_2O_5 are fixed and therefore independent of the bulk slag composition. The P_2O_5 activities in the four-phase assemblages of $Ca_3SiO_5 + Ca_2SiO_4 + \langle C_2S\text{-}C_3P\rangle ss + \text{Liquid}$, $CaO + Ca_3SiO_5 + \langle C_2S\text{-}C_3P\rangle ss + \text{Liquid}$ and $CaO + Ca_4P_2O_9 + Ca_5P_2SiO_{12} + \text{Liquid}$ are given by equations (27), (59) and (22), respectively. On the other hand, the FeO activities have been reported as follows /11/.

$$\log a_{FeO} = -0.77 + 720/(T/\text{K})$$
$$Ca_3SiO_5 + Ca_2SiO_4 + \langle C_2S\text{-}C_3P\rangle ss + \text{Liquid} \quad (77)$$

$$\log a_{FeO} = -1.57 + 1{,}960/(T/\text{K})$$
$$CaO + Ca_3SiO_5 + \langle C_2S\text{-}C_3P\rangle ss + \text{Liquid} \quad (78)$$

$$\log a_{FeO} = 0.90 - 1{,}810/(T/\text{K})$$
$$CaO + Ca_4P_2O_9 + Ca_5P_2SiO_{12} + \text{Liquid} \quad (79)$$

Figure 6 shows the estimated phosphorus contents in molten iron attainable with the four-phase assemblages under consideration. This figure also gives the final phosphorus levels achieved with the industrial slags, given in Table 3 /12/. It is evident from this graph that the phosphorus concentrations attainable by using the heterogeneous slags are four to five orders of magnitude lower than those obtained with the industrial slags. As a consequence of this behavior, the opportunity is available to considerably reduce required slag volume. Recently, phosphorus removal from hot metal in Japanese steelmaking industries has been operated with relatively lower basic slags to aim at reducing consumption of fluorspar, CaF_2, which causes emission of hazardous fluoride species. The present results of solid solutions between Ca_2SiO_4 and $Ca_3P_2O_8$ would also be applicable to estimate thermodynamic properties of such dephosphorization slags.

Sample Code	Slag composition (mole %)						Hot metal	
	CaO	SiO_2	FeO	CaF_2	P_2O_5	Others*	*T*/K	*[%P]*
#1	53.0	32.2	1.7	6.8	1.1	5.3	1548	0.112
#2	57.3	28.3	2.5	5.6	1.8	4.5	1548	0.090
#3	58.3	20.8	2.4	10.4	2.6	5.5	1548	0.057
#4	58.9	16.1	2.1	11.1	3.2	8.6	1548	0.016
#5	58.3	11.1	1.6	21.0	3.4	4.6	1573	0.020
#6	60.0	11.6	1.1	21.5	2.1	3.7	1543	0.030

* "Others" means $CaS + MgO + MnO + Al_2O_3$

Table 3: Industrial slags of hot metal processing and corresponding hot metal temperature and phosphorus level.

5 Conclusions

Solution models have been applied to solid solutions between Ca_2SiO_4 and $Ca_3P_2O_8$ to aim at deriving their thermodynamic properties at 1573 K. The parameters included in the regular solution model were determined under the conditions that the activities of Ca_2SiO_4 and $Ca_3P_2O_8$ were consistent with the literature data and the phase diagrams. The present results suggested the estimations of the activities of the components in the CaO-SiO_2-P_2O_5 ternary system at high CaO contents and the composition of the Ca_2SiO_4-$Ca_3P_2O_8$ solid solution in equilibrium with CaO and Ca_3SiO_5 at 1573 K.

Received: March 2, 2012. Accepted: July 10, 2012.

References

[1] M. Matsu-sue, M. Hasegawa, K. Fushi-tani and M. Iwase, *Steel Res. Int.*, **78** (6), 465–467 (2007).

[2] W. Fix, H. Heymann and R. Heinke, *J. Am. Ceram. Soc.*, **52** (6), 346–347 (1969). Cited from ACerS-NIST PHASE EQUILIBRIUM DIAGRAMS, CD-ROM database, Version 3.1, Figure 4563.

[3] H. Suito, Y. Hayashida and Y. Takahashi, *Tetsu-to-Hagané* (in Japanese), **63** (8), 1252–1259 (1977).

[4] O. Kubaschewski, C. B. Alcock and P. J. Spencer, *Materials Thermochemistry*, 6th edition, Pergamon Press, 1993.

[5] M. Hasegawa and M. Iwase, Private communication.

[6] H. Yama-zoye, E. Ichise, H. Fujiwara and M. Iwase, *Iron Steelmaker*, **18** (5), 75–80 (1991).

[7] M. Iwase, H. Fujiwara, E. Ichise, H. Kitaguchi and K. Ashida, *Iron Steelmaker*, **16** (4), 45–52 (1989).

[8] E. T. Turkdogan and J. Pearson, *J. Iron Steel Inst.*, **175**, 393–401 (1953).

[9] H. Takeshita, M. Hasegawa, Y. Kashiwaya and M. Iwase, *Steel Res. Int.*, **81** (2), 100–104 (2010).

[10] E. T. Turkdogan and J. Pearson, *Journal of the Iron and Steel Institute*, **175**, 393–401 (1953).

[11] M. Matsu-suye, K. Fushi-tani, M. Hasegawa and M. Iwase, *Steel Res. Int.*, **79** (9), 678–684 (2008).

[12] M. Iwase, N. Yamada, H. Akizuki and E. Ichise, *Arch. Eisenhüttenwes.*, **55**, 471–476 (1984).